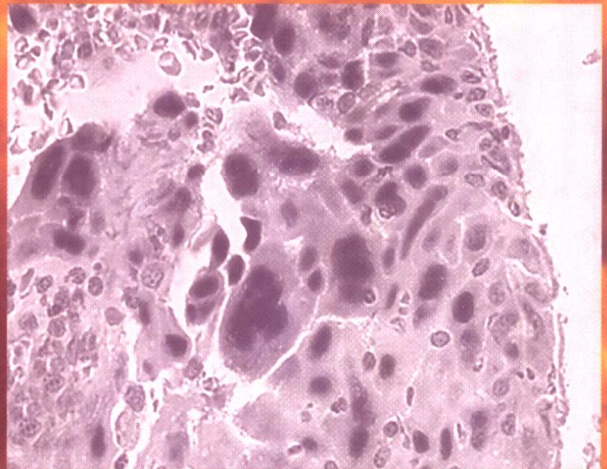# MORPHOLOGY METHODS

Cell and Molecular Biology Techniques

Edited by

RICARDO V. LLOYD, MD, PhD

Humana Press

MORPHOLOGY

METHODS

Cell and Molecular

Biology Techniques

Edited by

Ricardo V. Lloyd, MD, PhD

Mayo Clinic, Rochester, MN

Foreword by

Ronald A. DeLellis, MD

Weill Medical College of Cornell University and
New York Presbyterian Hospital, New York, NY

✳ **Humana Press**
Totowa, New Jersey

This publication is printed on acid-free paper. ∞

ANSI Z39.48-1984 (American Standards Institute) Permanence of Paper for Printed Library Materials.

Cover illustrations: Backround is figure 18 and inset is figure 5 from Chapter 4, "*In Situ* Detection of Infectious Agents," by Gary W. Procop and Randall Hayden.

Cover design by Patricia F. Cleary.

For additional copies, pricing for bulk purchases, and/or information about other Humana titles, contact Humana at the above address or at any of the following numbers: Tel: 973-256-1699; Fax: 973-256-8341; E-mail: humana@humanapr.com, or visit our Website: http://humanapress.com

Printed in the United States of America. 10 9 8 7 6 5 4 3 2 1

Foreword

The past several decades have witnessed an impressive array of conceptual and technological advances in the biomedical sciences. Much of the progress in this area has developed directly as a result of new morphology-based methods that have permitted the assessment of chemical, enzymatic, immunological, and molecular parameters at the cellular and tissue levels. Additional novel approaches including laser capture microdissection have also emerged for the acquisition of homogeneous cell populations for molecular analyses. These methodologies have literally reshaped the approaches to fundamental biological questions and have also had a major impact in the area of diagnostic pathology.

Much of the groundwork for the development of morphological methods was established in the early part of the 19th century by Francois-Vincent Raspail, generally acknowledged as the founder of the science of histochemistry. The earliest work in the field was primarily in the hands of botanists and many of the approaches to the understanding of the chemical composition of cells and tissues involved techniques such as microincineration, which destroyed structural integrity. The development of aniline dyes in the early 20th century served as a major impetus to studies of the structural rather than chemical composition of tissue. Later in the century, however, the focus returned to the identification of chemical constituents in the context of intact cell and tissue structure. Ultimately, it became possible to localize with great precision major classes of nucleic acids, proteins, and individual amino acids, lipids, and carbohydrates on the basis of specific chemical reactions that had been adapted for histological and cytological preparations.

The development of the immunofluorescence technique for the localization of pneumococcal antigens in 1942 by Albert Coons and his colleagues provided the foundation for the subsequent development of enzyme-based immunohistochemical procedures. The advantages of these methods were related to the facts that the reaction products could be visualized directly in the light microscope and that the multistep staining procedures possessed sufficient sensitivity to localize even the small amounts of antigen that survived formalin fixation and paraffin embedding. The subsequent development of increasingly more sensitive immunohistochemical staining sequences and the availability of increasing numbers of monoclonal antibodies together with the development of antigen retrieval technology has made immunohistochemistry clearly one of the most important research and diagnostic tools in the armamentarium of the investigator.

The development of molecular technologies has had an equally profound impact on approaches to the analysis of basic biological questions directly in tissue sections and single cells. *In situ* hybridization techniques, including FISH, have emerged as powerful techniques for the localization of DNA and RNA sequences at the cellular and subcellular levels. Increased sensitivity of *in situ* hybridization has been made possible both by amplification of target sequences through the use of the polymerase chain reaction (PCR) and *in situ* reverse transcriptase (RT)—PCR methods, as well as by approaches to enhance signal amplification, including the use of increasingly more sensitive nonradioactive techniques. Tissue and cDNA microarrays have provided a particularly useful approach for large scale analyses of DNA, RNA, or protein and for studies of gene expression.

The major objective of Dr. Lloyd's book is to present an overview of the major areas relevant to the current practice of molecular morphology. Both he and his distinguished group of contributors have been particularly successful in achieving this goal and in providing succinct overviews of specific methodologies, their major applications and detailed protocols for their performance.

Dr. Lloyd's monograph will undoubtedly find an important place on the bookshelves of basic scientists and clinical investigators who have an interest in correlating morphological and molecular parameters.

Ronald A. DeLellis, MD
Professor of Pathology
Weill Medical College of Cornell University
Vice Chair for Anatomic Pathology
New York Presbyterian Hospital
New York, NY

Preface

Molecular morphologic methods—defined as molecular and cell biologic analyses of tissues in which the architectural integrity and spatial interrelationship of the cells being studied are preserved—have increased rapidly in number and versatility during the past few years. These changes have occurred both in diagnostic pathology and in basic scientific research. Several ongoing developments affecting the pathology and the scientific communities should make this book a valuable resource. First, it is usually difficult for pathologists and investigators interested in molecular morphology to learn rapidly from a single source about methods suitable to specific diagnostic and experimental questions. Second, the completion of the human genome project in the near future will provide the foundation to learn about the functions of myriad of genes with unique roles in specific cells and tissues, so a morphologic basis for the study of human genes and understanding human diseases will be in greater demand. There is no good single source available that discusses in detail the most significant aspects of recent cell biologic techniques by outstanding experts in their fields. Such a book is needed to keep up with scientific research in morphology and recent pathologic diagnostic techniques relevant in the twenty-first century.

Our objective was to produce a book addressing the major areas relevant to molecular morphology today. Many of the chapters include detailed protocols for setting up or performing techniques now in use. Potential pitfalls and anticipated problems are also discussed. Practicing pathologists interested in recent developments and researchers interested in molecular morphology for designing experiments, for teaching undergraduate, graduate, and professional students, or simply for keeping up with the literature detailing molecular morphologic approaches—all will find here the technical and scientific background to accomplish their objectives.

The publication of *Morphology Methods: Cell and Molecular Biology Techniques* would not have been possible without the enthusiastic support and contributions of Mr. Thomas Lanigan, President, and Mr. John Morgan of Humana Press.

Ricardo V. Lloyd, MD, PhD

Contributors

- MUHAMMAD AMJAD, PhD • *Laboratories of Transgenic and Recombinant Vaccine, Department of Biology, Lincoln University, Lincoln University, PA*
- OMAR BAGASRA, MD, PhD • *Laboratories of Transgenic and Recombinant Vaccine, Department of Biology, Lincoln University, Lincoln University, PA*
- LISA E. BOBROSKI, MS • *Laboratories of Transgenic and Recombinant Vaccine, Department of Biology, Lincoln University, Lincoln University, PA*
- LISA A. CERILLI, MD • *Fechner Laboratory of Surgical Pathology, University of Virginia Medical Center, Charlottesville, VA*
- JOHN L. FRATER, MD • *Department of Clinical Pathology, Cleveland Clinic Foundation, Cleveland, OH*
- RANDALL HAYDEN, MD • *Clinical and Molecular Microbiology, St. Jude Children's Research Hospital, Cleveland, OH*
- EVA HORVATH, PhD • *Department of Laboratory Medicine, St. Michael's Hospital, University of Toronto, Toronto, Ontario, Canada*
- PHILIP N. HOWLES, PhD• *Department of Pathology and Laboratory Medicine, University of Cincinnati College of Medicine, Cincinnati, OH*
- ERIC D. HSI, MD • *Departments of Anatomic and Clinical Pathology, Cleveland Clinic Foundation, Cleveland, OH*
- JOHBU ITOH, MD, PhD • *Laboratories for Structure and Function Research, Tokai University School of Medicine, Boseidai, Isehara City, Kanagawa, Japan*
- JIN LONG • *Mayo Clinic and Foundation, Rochester, MN*
- NIKIFOROS KAPRANOS, MD, PhD • *Department of Pathology, Molecular Division, Amalia Fleming Hospital, Athens, Greece*
- PAUL KOMMINOTH, MD • *Department of Pathology, Hospital Baden, Baden, Switzerland*
- GEORGE KONTOGEORGOS, MD, PhD • *Department of Pathology, G. Gennimatas General Hospital of Athens, Athens, Greece*
- KALMAN KOVACS, MD, PhD • *Department of Laboratory Medicine, St. Michael's Hospital, University of Toronto, Toronto, Ontario, Canada*
- PAUL J. KURTIN, MD • *Divisions of Anatomic Pathology and Hematopathology, Mayo Clinic, Rochester, MN*
- LARS-INGE LARSSON, DSc • *Division of Cell Biology, Department of Anatomy and Physiology, The Royal Veterinary and Agricultural University, Frederiksberg, Denmark*
- RICARDO V. LLOYD, MD, PhD • *Department of Laboratory Medicine and Pathology, Mayo Clinic and Foundation, Rochester, MN*

- AKIRA MATSUNO, MD, PhD • *Department of Neurosurgery, Teikyo University Ichihara Hospital, Ichihara City, Chiba, Japan*
- TADASHI NAGASHIMA, MD, PhD • *Department of Neurosurgery, Teikyo University Ichihara Hospital, Ichihara City, Chiba, Japan*
- YURI E. NIKIFOROV, MD, PhD • *Department of Pathology and Laboratory Medicine, Univeristy of Cincinnati College of Medicine, Cincinnati, OH*
- R. YOSHIYUKI OSAMURA, MD, PhD • *Department of Pathology, Tokai University School of Medicine, Boseidai, Isehara City, Kanagawa, Japan*
- AUREL PERREN, MD • *Department of Pathology, University Hospital Zürich, Zürich, Switzerland*
- GARY W. PROCOP, MD • *Clinical Microbiology, Cleveland Clinic Foundation, Cleveland, OH*
- XIANG QIAN • *Mayo Clinic and Foundation, Rochester, MN*
- PATRICK C. ROCHE, PhD • *Department of Laboratory Medicine and Pathology, Mayo Clinic, Rochester, MN*
- NAOKO SANNO, MD, PhD • *Department of Neurosurgery, Nippon Medical School, Tokyo, Japan*
- SUSAN SHELDON, PhD • *Department of Pathology, University of Michigan, Ann Arbor, MI*
- SHAN-RONG SHI, MD • *Department of Pathology, Keck School of Medicine, University of Southern California, Los Angeles, CA*
- CLIVE R. TAYLOR, MD, PhD • *Department of Pathology, Keck School of Medicine, University of Southern California, Los Angeles, CA*
- AKIRA TERAMOTO, MD, DMSc • *Department of Neurosurgery, Nippon Medical School, Tokyo, Japan*
- ELENI THODOU, MD, PhD • *Department of Pathology, G. Gennimatas General Hospital of Athens, Athens, Greece*
- RAYMOND R. TUBBS, DO • *Department of Clinical Pathology, Cleveland Clinic Foundation, Cleveland, OH*
- SERGIO VIDAL, DVM, PhD • *Department of Laboratory Medicine, St. Michael's Hospital, University of Toronto, Toronto, Ontario, Canada; Laboratory of Histology, University of Santiago de Compostela, Lugo, Spain*
- KEIICHI WATANABE, MD, PhD • *Department of Pathology, Tokai University School of Medicine, Boseidai, Isehara City, Kanagawa, Japan*
- MARK R. WICK, MD • *Fechner Laboratory of Surgical Pathology, University of Virginia Medical Center, Charlottesville, VA*

Color Plates

Color Plate 1 *Fig. 1, Chapter 3.* (**A**) *In situ* hybridization detects EBV in a posttransplant lymphoproliferative disorder. (**B**) *In situ* hybridization to detect EBV in a nasopharyngeal carcinoma metastatic to a cervical lymph node. (**C**) Detection of κ (left) and λ (right) in a plasmacytic lymphoma. (**D**) *In situ* hybridization for albumin to diagnose a hepatocellular carcinoma metastatic to the scapula. (**E**) Chromogranin A and B expression in the adrenal cortex. (**F**) Pro-insulin mRNA expression in the normal pancreatic islets. *See* discussion on pages 36, 39 and full caption on page 37.

Color Plate 2 *Figs. 1–19, Chapter 4. See* pages 47–55. • *Fig. 1.* Lymph noted with EBV, ISH. • *Fig. 2.* Pharyngeal biopsy with HPV, ISH. • *Fig. 3.* Placenta, involved by CMV, ISH. • *Fig. 4.* Oral cavity (palate) biopsy with HSV, H&E. • *Fig. 5.* Palate biopsy with HSV (*Fig. 4*) confirmed by ISH. • *Fig. 6.* Lung tissue with adenovirus, H&E. • *Fig. 7.* Adenovirus in lung tissue (*Fig. 6*) confirmed by ISH. • *Fig. 8.* Brain biopsy showing JC viral inclusion in oligodendrocytes, H&E. • *Fig. 9.* JC virus in brain biopsy (*Fig. 8*) confirmed by ISH. • *Fig. 10. Cryptococcus neoformans* in an open lung biopsy, GMS. • *Fig. 11.* Identification of the yeast forms in *Fig. 10* as *C. neoformans* using ISH. • *Fig. 12. Histoplasma capsulatum* in an open lung biopsy, GMS. • *Fig. 13.* Confirmation of the yeast forms in *Fig. 12* as *H. capsulatum* using ISH. • *Fig. 14.* Open lung biopsy with *Blastomyces dermatiditis*, GMS. • *Fig. 15.* Confirmation of the yeast forms in *Fig. 14* with ISH. • *Fig. 16.* Endospores and immature spherules of *Coccidiodes immitis* in a lung biopsy, GMS. • *Fig. 17.* Confirmation of *C. immitis* in *Fig. 16* by ISH. • *Fig. 18.* Open lung biopsy showing *Legionella pneumophila*, Warthin-Starry stain. • *Fig. 19.* Identification of *L. pneumophila* in *Fig. 18* by ISH.

Color Plate 3 *Figs. 5, 6, and 7, Chapter 5. See* pages 74–79 for discussion and additional details. • *Fig. 5.* Two-color microdeletion probe. • *Fig. 6.* A two-color probe for *BCR* and *ABL* genes on a touch preparation from a spleen. • *Fig. 7.* Painting probe for chromosome 9.

Color Plate 4 *Fig. 3, Chapter 6. See* pages 94–95. (**A**) Examples of numerical chromosome aberrations using an α-satellite, centromere-specific DNA probe. (**B**) Monosomy of chromosome 11 as the dominant abnormality in a mixed somatotrophlactotroph, mostly prolactin-producing pituitary adenoma (FITC/PI). (**C**) Chromosome 1 in ductal carcinoma of the breast. (**D**) Chromosome 2 breast carcinoma of the ductal type. (**E**) Localization of the DiGeorge gene on a chromosome in the 22q11 region in normal metaphase spreads. (**F**) Dual-color FISH in metaphases of normal lymphocytes demonstrates the *bcr* gene on chromosome 22 (green) and the *abl* gene on chromosome 9 (red) (FITC/TR/DAPI). (**G**) Mixture of whole paint (coatsome) DNA probe for chromosome 11 (red) and α-satellite centromere-specific probe or chromosome 2 (green) in normal metaphase spreads (FITC/TR/DAPI). (**H**) All human telomeres demonstrate all chromosomes in metaphase spreads (FITC/PI).

Color Plate 5 *Figs. 9 and 10,* Chapter 10. • *Fig. 9.* Three-dimensional projection images of ACTH and GH cells in normal rat pituitary. (**A**) ACTH cells are closely associated with the microvessel networks. (**B**) ACTH signals show a granular pattern in the cytoplasm. (**C**) GH cells are clearly visible three-dimensionally by CLSM reflectance mode. (**D**) GH signals appear granular in the cytoplasm three-dimensionally by CLSM reflectance mode. See discussion on page 174 and full caption on page 176. • *Fig. 10.* Three-dimensional reconstructed images of bilaterally adrenalectomized and ACTH administered rat pituitary glands. *See* discussion on pages 174–175 and full caption on page 177.

Color Plate 6 *Figs. 1–5, Chapter 16.* • *Fig. 1.* Immunoperoxidase stains for κ (**A**) and λ (**B**) immunoglobulin light chains on frozen section of a case of B-cell small lymphocytic lymphoma. *See* discussion and full caption on pages 280, 281. • *Fig. 2.* Immunoperoxidase stains for κ (**A**) and λ (**B**) immunoglobulin light chains on paraffin sections of a case of mantle cell lymphoma. *See* discussion on page 280 and full caption on page 282.• *Fig. 3.* B-cell small lymphocytic lymphoma. H&E section demonstrating the typical cytologic features (**A**). Frozen section immunoperoxidase stains for CD20 (**B**), CD5 (**C**), CD3 (**D**), and CD23 (**E**). *See* discussion on page 283 and full caption on page 284. • *Fig. 4.* Angioimmunoblastic T-cell lymphoma stained in frozen sections for CD2 (**A**) and for CD7 (**B**). *See* discussion on page 286 and full caption on page 287. • *Fig. 5.* Follicular lymphoma stained for bcl-2 paraffin sections. *See* discussion on page 288 and full caption on page 289.

Color Plate 7 *Figs. 6–13, Chapter 16.* • *Fig. 6.* Mantle cell lymphoma stained for cyclin D1 in paraffin sections. *See* discussion and full caption on pages 289, 290. • *Fig. 7.* CD30-positive anaplastic large cell lymphoma stained for p80 paraffin sections. *See* discussion and full caption on pages 290, 291. • *Fig. 8.* Diffuse large B-cell lymphoma involving a lymph node. H&E section (**A**) and immunoperoxidase stain (**B**). *See* discussion and full caption on pages 292, 293. • *Fig. 9.* Angioimmunoblastic T-cell lymphoma involving a lymph node. H&E section (**A**) and immunoperoxidase stain (**B**) for CD3 performed on a paraffin section of the tumor. *See* discussion and full caption on pages 294, 295. • *Fig. 10.* Immunoperoxidase stain for CD10 performed on a paraffin section of a follicular lymphoma. *See* discussion and full caption on pages 296, 297. • *Fig. 11.* Immunoperoxidase stain for CD23 performed on a paraffin section of an angio-immunoblastic T-cell lymphoma. Same case as *Fig. 9. See* discussion and full caption on pages 298, 299. • *Fig. 12.* Immunoperoxidase stain performed on a paraffin section for the cytolytic granule protein Tia-1 in a case of NK/T-cell lymphoma of the nasal type. *See* discussion and full caption on pages 298, 299. • *Fig. 13.* Immunoperoxidase stain for CD30 performed on a CD30-positive anaplastic large cell lymphoma. *See* full caption and discussion on pages 300, 301.

Color Plate 8 *Figs. 14–19, Chapter 16* • *Fig. 14.* Hodgkin's lymphoma, nodular sclerosis type involving a lymph node. H&E section demonstrating the large neoplastic cells admixed with small lymphocytes, eosinophils, plasma cells, and macrophages (**A**). Immunoperoxidase stains for CD15 (**B**), CD30 (**C**), and fascin (**D**) performed on paraffin sections. *See* discussion and full caption on pages 301–303. • *Fig. 15.* Hodgkin's lymphoma, nodular lymphocyte predominance type, involving a lymph node. *See* discussion on pages 302, 304, and full caption on page 305. • *Fig. 16.* Acute lymphoblastic leukemia, B-lymphocyte precursor type. *See* discussion and full caption on pages 305, 306. • *Fig. 17.* Acute myelogenous leukemia, FAB subtype M1. *See* discussion and full caption on pages 306, 307. • *Fig. 18.* Langerhans' cell histiocytosis involving the parotid gland. H&E (**A**) exhibits the typical cytologic features of this disorder. Immunoperoxidase stain for CD1a (**B**) performed in paraffin sections. *See* discussion and full caption on pages 307, 308. • *Fig. 19.* Histiocytic sarcoma. Immunoperoxidase stains for CD45 (**A**) and CD68 (**B**), in paraffin sections, and for CD13 on frozen sections of the tumor (**C**). *See* discussion on page 308 and full caption on page 309.

Contents

Introduction to Molecular Methods

Ricardo V. Lloyd, MD, PhD

GENE STRUCTURE

The human genome contains 23 pairs of chromosomes with 3.5×10^9 nucleotide base pairs (bp) in length. With the near completion of the sequencing of the human gene, the best estimate of functional genes appears to be between 30,000 and 40,000 *(1–3)*. Approximately 90% of the human DNA has no known coding function, but a significant amount of DNA, especially in regions close to functional genes, has regulatory roles in cells. However, most of the functions of much of the DNA remain unknown.

Specific restriction enzymes derived from prokaryotes are used to cleave DNA at specific sequences, which helps in the analysis of the large amount of genomic DNA. For example, EcoRI, which is derived from *Escherichia coli,* cleaves DNA at the G↓ AATTC sequence. Because of the specificity of restriction endonucleases, the DNA can be manipulated by genetic engineering, since DNA from any source cut by EcoRI will produce identical ends that hybridize to any other source of DNA produced by digestion with these restriction enzyme *(4,5)*.

CHEMICAL COMPOSITION OF NUCLEIC ACIDS

DNA and RNA are made of nucleotides, sugars, and phosphate groups (**Figs. 1–3**). DNA has four bases, the purines adenine and guanine and the pyrimidines cytosine and thymine. In RNA molecules, uracil is substituted for cytosine. The bases are linked to sugar groups (nucleoside), which are in turn linked to phosphates (nucleotides).

DNA and RNA are polynucleotide molecules with alternating series of sugar and phosphate groups (**Fig. 1**). The nucleotide sequences of a polynucleotide is usually written in the 5′ to 3′ order. The nucleotide sequence of DNA contains the genetic information.

The four DNA polynucleotide structures are base-paired in a complementary and parallel manner (**Fig. 2**). One strand runs from 3′ to 5′, and the other strand runs from 5′ to 3′. The DNA structure is twisted in a helix with one complete turn every three base pairs. During hybridization, which is one of the basic tools in molecular analyses, the two strands anneal or come together by base-pairing.

Humans somatic cells contain 46 chromosomes, which are made up of 23 pairs. The 23 pairs represent the haploid number of chromosomes, and the 46 chromosomes
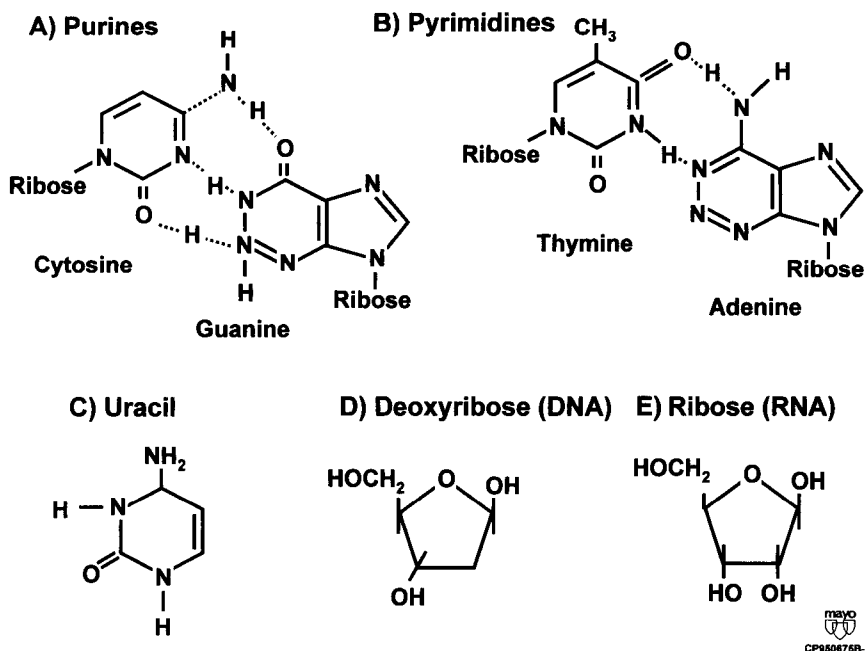
Fig. 1. Structure of molecules making up DNA and RNA. The bases (cytosine, guanine, thymine, adenine, and unacil) are linked via hydrogen bonds. (**A**) The purines are linked by three pairs of hydrogen bonds. (**B**) The pyrimidines are linked by two pairs of hydrogen bonds. (**C**) The structure of unacil, present in RNA in place of thymine. (**D**) and (**E**) Structures of the pentose sugars in DNA and RNA.

represent the diploid number, which represents the two homologous sites of each chromosome.

The sex chromosomes are different in males and females; females have two X chromosomes, and males have a Y and an X chromosome. The karyotype represents the complete chromosomal complement of a cell. These karyotypes are usually analyzed by cytogeneticists. Chromosomes are linked by a centromere with two sister chromatid portions. Chromosome maps are based on the position of the banding pattern (easily visualized after staining with specific dyes) and the position of the centromeres. Chromosomes are numbered as 1–22 plus the sex chromosomes. The short arm of the chromosomes is designated as a p and the long arm as q. The p and q arms are divided into various sections. Thus a designation of 5q21 would represent the long arm of chromosome 5, section 2, and band 1 (**Fig. 4**).

RNA AND PROTEIN SYNTHESIS

Transcription is the process by which RNA is synthesized from DNA (**Fig. 5**). The RNA is complementary to the original DNA strand. RNA is synthesized 5′–3′ by RNA polymerases. There are different forms of RNA. For example, transfer RNA, small nuclear RNA, and ribosomal RNA are end products of transcription. In contrast, messenger RNA (mRNA) constitutes most of the RNA that encodes specific protein products
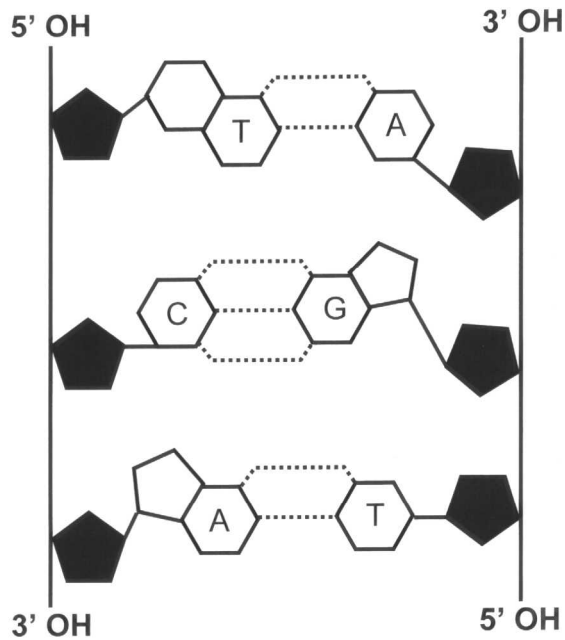
Fig. 2. Structure of double-stranded DNA. The deoxyribonucleotide residues (black areas) of each single strand of DNA are linked by phosphodiester bonds between the 3′ carbon of the first deoxyribose residue and the 5′ carbon of the next residue. The purines and pyrimidines are linked by hydrogen bonds. The two DNA strands are on antiparallel orientations.
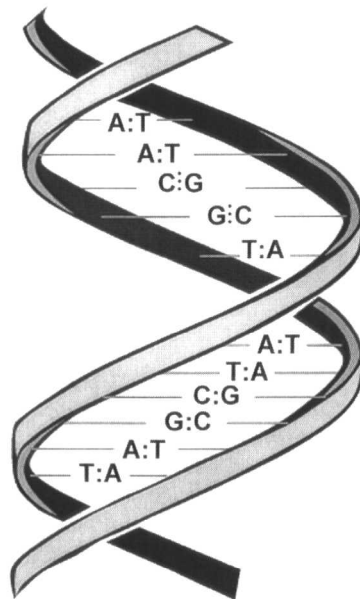

Fig. 3. Structure of the double helix, showing the three-dimensional relationship among the bases, sugars, and phosphodiester moieties.
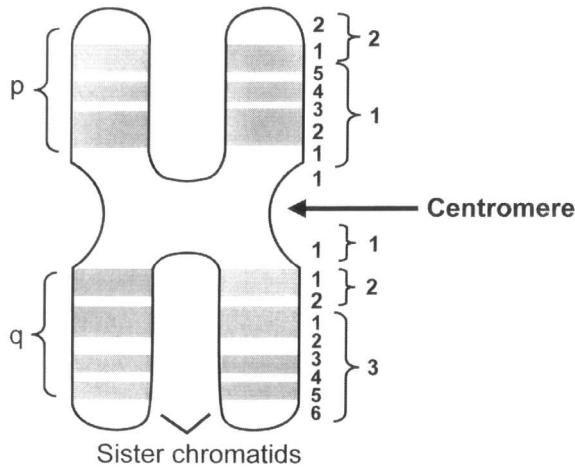
Fig. 4. Physical map of chromosome 7 after Giemsa staining and G-banding. Giemsa staining highlights the dark and light bands. The centromere and sister chromatids are shown.
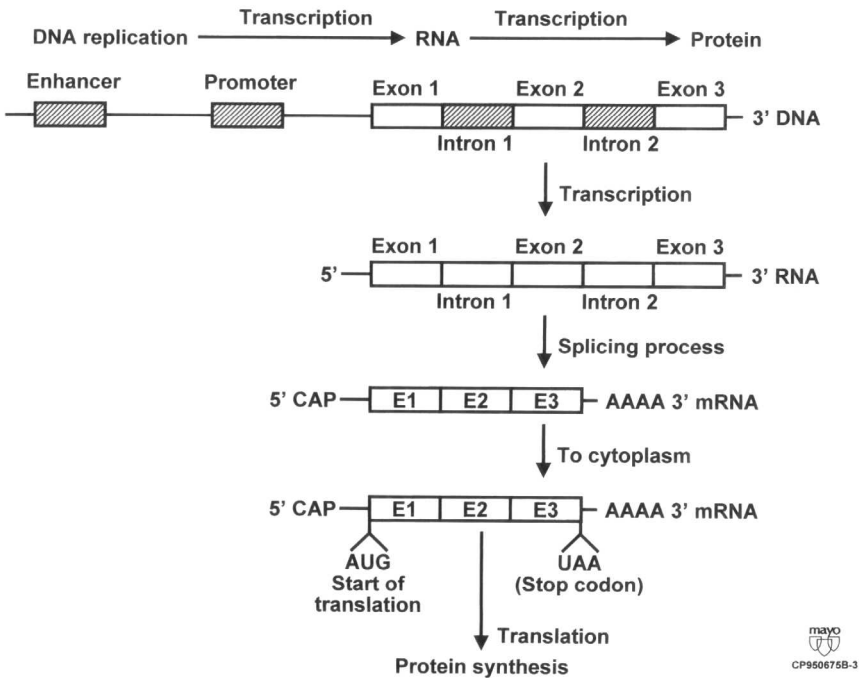

Fig. 5. Diagrammatic representation of transcription and translation processes leading to specific protein synthesis. The regulatory sequence with the enhancer and promoter sequences are located in the 5′ upstream region. Enhancers bind protein factors and help to determine the rate of transcription. The coding sequences downstream include exons and introns. Introns are spliced out of the mature RNA. AUG is the start codon for protein coding, and there are three stop codons to terminate protein synthesis (UAA, UAG, and UGA). The 5′ CAP site is at the 5′ end, and the poly(A) tail is present at the 3′ end. These sites help to increase the stability of the mature mRNA and optimize protein synthesis.